



Editor's choice paper

Oxidation of styrene and of some derivatives with H₂O₂ catalyzed by novel imidazolium-containing manganese porphyrins: A mechanistic and thermodynamic interpretation

Rodrigo De Paula*, Mário M.Q. Simões, M. Graça P.M.S. Neves, José A.S. Cavaleiro**

Department of Chemistry & QOPNA, University of Aveiro, 3810-193 Aveiro, Portugal

ARTICLE INFO

Article history:

Received 11 March 2011

Accepted 18 May 2011

Available online 26 May 2011

Keywords:

Manganese

Imidazolium porphyrins

Hydrogen peroxide

Oxidation

Eyring

Hammett

ABSTRACT

The oxidation of styrene and derivatives with H₂O₂ catalyzed by manganese porphyrins in acetonitrile is described. The effect of the imidazolium substituent on the catalytic efficiency has been also considered. The thermodynamic analysis has indicated that enthalpy rules styrene oxidation when catalysts **Mn(Porph)-1** and **Mn(Porph)-2** are used whereas the entropy is the driven force for **Mn(Porph)-3** and **Mn(Porph)-4** catalyzed reactions. Interestingly, an enthalpy–entropy compensation phenomenon is observed when comparing the thermodynamic results obtained for catalysts **Mn(Porph)-3** and **Mn(Porph)-4**. Hammett plots for the studied manganese porphyrins provided small ρ -values, and this is typical for multi-step reactions, indicating that there is no significant charge separation in the transition state. For **Mn(Porph)-1** and **Mn(Porph)-2** the formation of multiple active species can be put forward whereas for **Mn(Porph)-3** and **Mn(Porph)-4** a concerted-type mechanism, via metalloxetane intermediate, fits well with the values obtained for those catalysts. The imidazolium-based catalysts have shown to be efficient catalysts in styrene and derivatives oxidation with hydrogen peroxide.

© 2011 Elsevier B.V. All rights reserved.

1. Introduction

Olefins epoxidation is a transformation intensively investigated over the years and this is mainly due to the resulting epoxides' applications and also for ascertaining mechanistic aspects in metal catalyzed reactions [1–3].

Epoxidations can be performed by a great variety of transition-metal complexes (such as Ta, V, Ti, Hf and others) [4], but an elegant strategy consists in developing biomimetic or bioinspired catalysts based on a detailed knowledge of enzymatic systems, particularly that of the cytochrome P450 family [5–12].

Studies devoted to epoxidation reactions catalyzed by synthetic metalloporphyrins have made clear that iron and manganese porphyrin complexes are excellent catalytic models [4,13–16] of biologically relevant iron (*i.e.* cytochromes) and manganese-containing enzymes [4,16,17]. They can act as biomimetic *monooxygenase* or as *superoxide dismutase* enzymes and the modulation of one or the other pathway can be achieved by the correct

choice of the fifth ligand [12,16]. This additive is needed to stabilize the oxo-metallocomplex formed during the reaction as well as to assist the substrate hydrogen abstraction [18–21] and the heterocyclic cleavage in hydroperoxy oxidants [12,16,22–26], resembling the biological function of the cysteinyl residue in cytochrome P450 *monooxygenase* enzymes.

It is now generally accepted that these reactions occur with the participation of high-valent oxo-metal species which can be generated by the interaction of the metalloporphyrin with oxygen donors such as hydrogen peroxide, alkyl hydroperoxides, iodosylarenes, sodium hypochlorite, potassium monopersulfate, amine *N*-oxides, peracids and others [17,27]. Many of the kinetic studies devoted to the elucidation of metalloporphyrin-catalyzed olefin epoxidation mechanisms have been hampered by competing side reactions and the insolubility of terminal oxidants [28,29]. Hydrogen peroxide has been used to overcome the solubility problems found with other common oxidant agents and has the advantage, by any criteria, to be a green, clean and cheap oxidant. The main problems in using hydrogen peroxide as oxidant are related to the metalloporphyrin stability towards the reaction conditions [30,31] and its dismutation (*catalase* pathway) [32,33]. Some publications highlight the importance of catalyst stability in hydrogen peroxide oxidations [34,35], but many studies have simply not considered or circumvented this problem by performing the reactions in the presence of an excess of substrate relatively to the amount of hydrogen peroxide used [36,37].

* Corresponding author. Present address: Universidade Federal do Recôncavo da Bahia – Centro de Formação de Professores, 45.300-000 Amargosa/BA, Brazil. Tel.: +55 75 3634 3042/+351 234370717; fax: +55 75 3634 3703/+351 234370084.

** Corresponding author. Tel.: +351 234370717; fax: +351 234370084.

E-mail addresses: rodrigodepaula@ua.pt, rodrigodepaula@ufrb.edu.br (R. De Paula), msimoes@ua.pt (M.M.Q. Simões), gneves@ua.pt (M.G.P.M.S. Neves), jcavaleiro@ua.pt (J.A.S. Cavaleiro).

Styrene, a key component in chemical industry [2], is also one of the most widely used substrates to study epoxidation reaction mechanisms by synthetic oxo-metalloporphyrin catalysts and by wild-type P450 enzymes [29,38–40]. The conversion of styrene into the epoxide, however, is not always a clean reaction since undesired side products, such as phenylacetaldehyde, can be formed. In some cases, benzaldehyde is also observed as a by-product and its formation is usually associated with radical processes [39,40].

Mechanistic studies have suggested that the reaction is stepwise or involves a stepwise branch with an intermediate that generates the by-products (Scheme 1). Two types of reaction intermediates, radicals and carbocations, are usually invoked to account for the side product formation (Scheme 1, species II, III and IV), while the stereospecific epoxidation is thought to occur by a concerted oxygen transfer mechanism (Scheme 1, species V). Studies on the epoxidation of styrene and styrene derivatives using synthetic catalysts have revealed a wealth of information. For example, *para*-substituted styrenes with electron-withdrawing groups enhance the epoxide/phenylacetaldehyde ratio, indicating the involvement of a cationic species such as those observed by Mansuy and collaborators in studies concerned with heme and non-heme based catalysts [41]. However, other researchers [42] believe that the resulting phenylacetaldehyde might come from the epoxide rearrangement assisted by the catalyst. Unlike the previous proposals, Collman et al. [43] observed that the amount of phenylacetaldehyde is constant with time, thus standing that both, epoxide and phenylacetaldehyde, might come from a common intermediate (via $\pi_{2a} + \pi_{2s}$ cycloaddition) (Scheme 1, species I).

DFT studies [39] using Compound I ([FeIV=O(protoporphyrin IX)^{•+}] coordinated with a thiolate residue) suggest that a multi-scenario can be found in C=C oxygenation and the authors have postulated the Multi-State Reactivity (MSR) Theory, which explains that depending on the catalyst, the substrate and the reaction conditions, a cationic and/or a radical species can be generated thus giving rise to the products observed.

Several studies on the use the metallocomplexes of tetra-substituted porphyrins as synthetic catalysts to understand the catalytic mechanism have been carried out. Normally, the *o,o'*-phenyl-substituted derivatives were required to perform those catalytic transformations, being the *chloro*[5,10,15,20-tetrakis-(2,6-dichlorophenyl)porphyrinato]manganese(III), **Mn(Porph)-1** (Scheme 2B), a well-known example of the second generation of metalloporphyrin catalysts. Scarce are the publications describing the use of porphyrinic ligands containing other *meso*-substituent rather than the conventional six-membered ring (phenyl, pyridyl and their substituted derivatives). In order to create and explore different structures, recent reports dealt with the use of some porphyrin derivatives containing imidazol-2-yl-type as *meso*-substituents. It is worth mentioning the work developed by Kobuke and co-workers [44] reporting the use of a series of unsymmetrical iron porphyrins based on an imidazolyl substituent at the *meso*-position in the oxidation of 2,4,6-tri-*t*-butylphenol by phenylperacetic acid. We have also reported the use of the manganese complex of a tetraimidazolium porphyrin in the epoxidation of olefins with H₂O₂ [45]. The latter are pioneer publications employing five-membered rings as *meso*-substituents of the porphyrin macrocycle.

Following this trend in developing new porphyrinic derivatives to get insight how to mimic nature, our proposal here is to analyze the results obtained in the oxidation of styrene and its derivatives with H₂O₂ (Scheme 2(A)) catalyzed by a series of imidazolium *meso*-substituted cationic manganese porphyrins (Scheme 2(B)) in comparison with the results obtained for the robust and well-studied Mn(TDCPP)Cl (herein named as **Mn(Porph)-1**). Also, using a simple mathematical treatment based on the steady-state

approach, it is aimed to understand the thermodynamics involved in the transition state of such oxidative processes.

2. Experimental

2.1. Synthesis of the free-base porphyrins

The syntheses of the starting porphyrins were carried out by following the typical Rothmund pyrrole and aldehyde condensation. For the symmetric compounds (**H₂-TDCPP** and **H₂-TMImP**), the used procedure was based on a methodology described by our group, using microwave irradiation [46]. The unsymmetric porphyrins (**H₂-3DC1MImP** and **H₂-1DC3MImP**) were obtained using a literature synthetic approach, based on the correct stoichiometric amount of each aldehyde and pyrrole in boiling acetic acid/nitrobenzene solution [47]. The porphyrins' metallation was carried out using MnCl₂·4H₂O in refluxing DMF [14]. Methylations of the manganese complexes were made in dry DMF using a large excess of iodomethane (150 equiv.). The experimental conditions were the same as described before [48] but under microwave irradiation for 1 h at 50 °C, using 800 W as the initial power (the detailed experimental procedure can be seen in Section S6 and Scheme S1 of the supporting information).

2.2. Free-bases and metallocomplexes characterization

The results obtained for ¹H NMR and mass spectrometry (MALDI TOF/TOF) for the symmetric starting porphyrins (**H₂-TDCPP** and **H₂-TMImP**) are in agreement with literature results [49,50] as well as for their metallocomplexes [49,51].

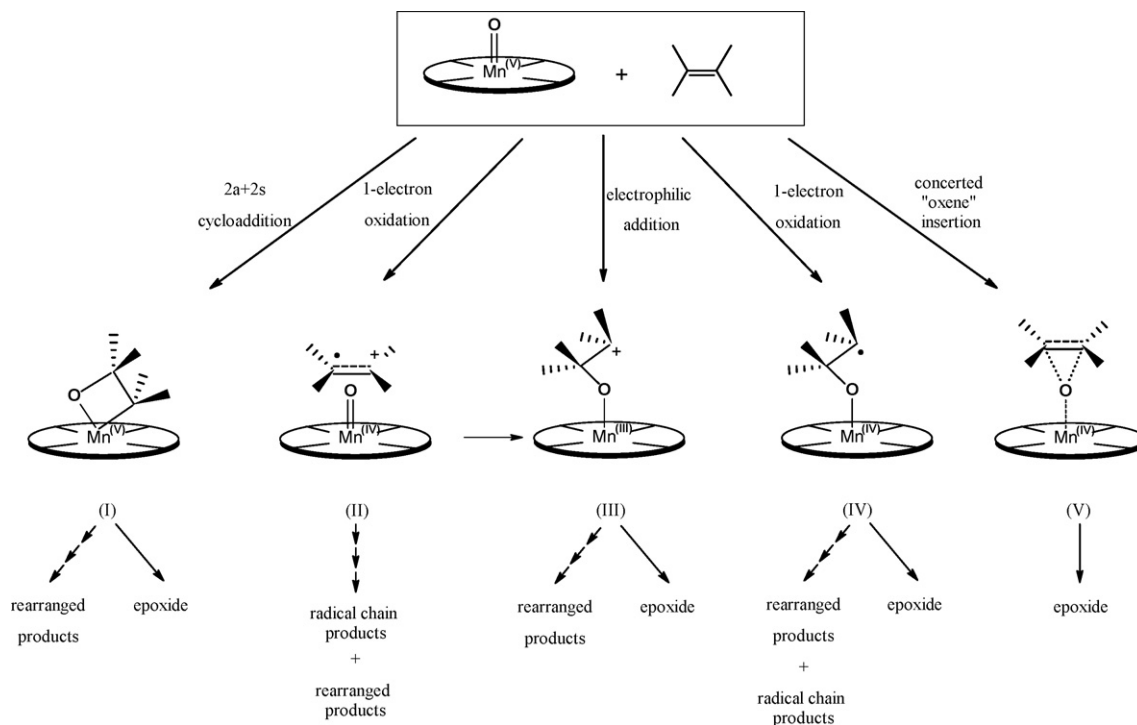
For the asymmetric free-base starting porphyrins (**H₂-3DC1MImP** and **H₂-1DC3MImP**) ¹H NMR spectroscopy and mass spectrometry (MALDI TOF/TOF) were used. For their corresponding neutral manganese complexes, MALDI TOF/TOF results are presented and for their cationic derivatives, the MALDI TOF/TOF and UV–Vis analysis are considered. The melting points of all compounds are higher than 300 °C.

H₂-3DC1MImP: ¹H NMR (CDCl₃, TMS as internal standard) δ /ppm: –2.63 (2H, s, N–H), 3.46 (3H, s, N–CH₃), 7.48 (1H, br. s, imidazole-H₄), 7.61 (1H, br. s, imidazole-H₅), 7.67–7.79 (9H, m, phenyl-H), 8.69–8.78 (8H, m, pyrrole- β H). ¹³C NMR (CDCl₃, TMS as internal standard) δ /ppm: 34.6 (N–CH₃), 114.4, 114.7, 115.1, 121.8 (Imidazole-C₅), 122.8, 127.6–127.9, 130.1, 130.5, 138.3–138.9. The mass analysis (MALDI TOF/TOF) gave 827.1 Da and the HRMS (ESI) analysis provided a peak at 823.02664 Da, assigned to [M+H]^{•+}, which is in good agreement with the expected formula C₄₂H₂₅N₆Cl₆ (822.0 Da).

H₂-1DC3MImP: ¹H NMR (CDCl₃, TMS as internal standard), δ /ppm: –2.83 and –2.78 (2H, 2s, N–H), 3.37–3.56 (9H, m, N–CH₃), 7.49 (d, *J* = 3.88 Hz, 3H, imidazole-H₄), 7.68 (d, *J* = 4.95, 3H, imidazole-H₅), 7.73–7.86 (3H, phenyl-H), 8.70–8.76 and 8.84–8.89 (8H, m, pyrrole- β H). ¹³C NMR (CDCl₃, TMS as internal standard) δ /ppm: 34.8, 34.9 (N–CH₃), 106.9, 107.1 and 107.2 (*meso*), 116.3, 122.4, 122.5, 122.6 127.976, 128.119, 128.140, 128.189, 128.213, 128.285, 128.336, 128.411, 128.468, 131.234, 131.374, 138.483, 138.630, 138.798, 147.575 (Imidazole-C₂), 147.614 (Imidazole-C₂). The mass analysis (MALDI TOF/TOF) for the calculated formula C₃₈H₂₈N₁₀Cl₂ (694.187546 Da) gave 697.2 Da as the main peak assigned as [M+H]^{•+} showing the typical chlorine isotope effect. The HRMS (ESI) analysis gave 695.19482 Da.

The mass analyses (MALDI TOF/TOF) for all the neutral metalloporphyrins' complexes gave the [M]^{•+} ions as expected:

Mn(Porph)-1: MALDI (TOF/TOF): [M+H]^{•+} = 942.8 Da and the HRMS (ESI) analysis provided a peak at 938.85712 Da, corresponding to the expected formula MnC₄₄H₂₀Cl₈N₄. UV–Vis spectroscopic



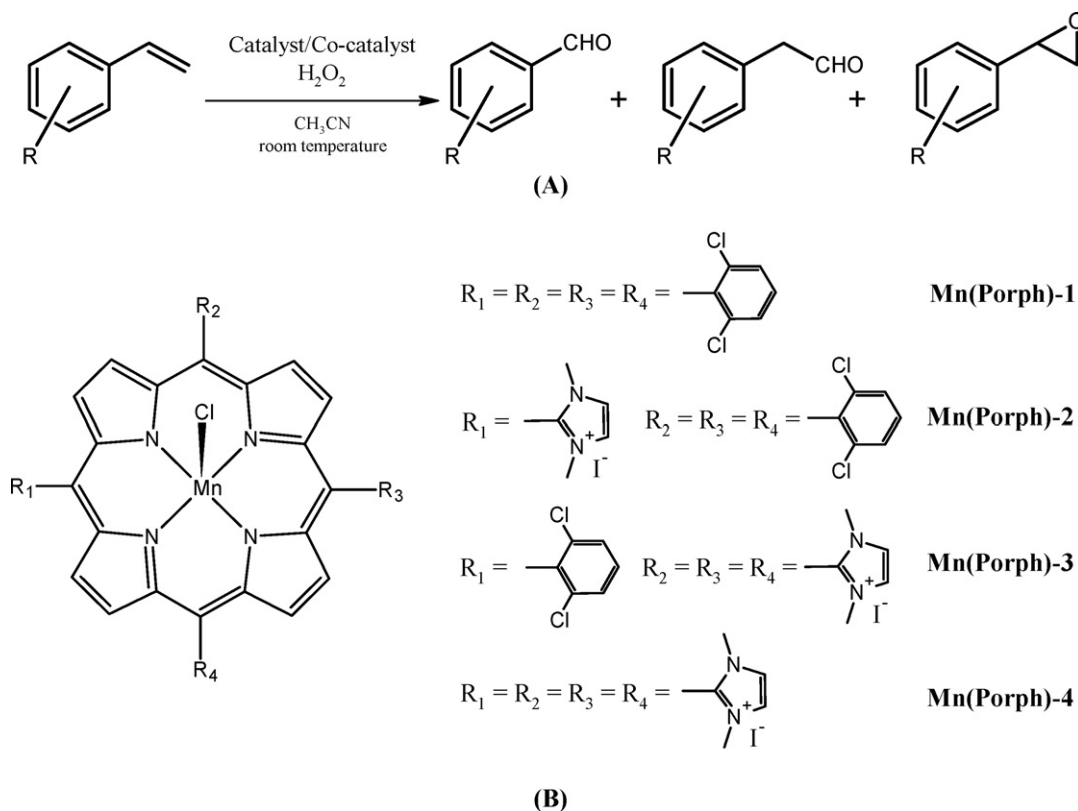
Scheme 1. Possible intermediates in alkene catalyzed oxidation in the presence of manganese porphyrins, according to Bruice and co-workers [62].

data, taken in CH_3CN : λ , nm ($\log \epsilon$): 369 (4.78), 476 (5.13), 579 (4.10), 614 (*sh.*, 3.73).

Mn(3DCP1MImP)Cl: MALDI (TOF/TOF): $[\text{M}+\text{H}]^+ = 878.9$ Da and HRMS (ESI): 874.94121 Da, in agreement with $\text{MnC}_{42}\text{H}_{22}\text{Cl}_6\text{N}_6 = 874.94176$ Da. A peak at 1755.8 Da in MALDI

(TOF/TOF) is assigned a dimer. UV–Vis spectroscopic data, taken in $\text{CH}_3\text{CH}_2\text{OH}$: λ , nm ($\log \epsilon$): 371 (4.41), 395 (4.38), 462 (4.89), 560 (3.86), 775 (3.07).

Mn(Porph)-2: MALDI (TOF/TOF): $[\text{M}]^+ = 891.9$ Da and HRMS (ESI): 889.96469 Da, in agreement with



Scheme 2. (A) Styrene and styrene derivatives catalyzed oxidation and products distribution and (B) catalysts used in this study.

$\text{MnC}_{43}\text{H}_{25}\text{Cl}_6\text{N}_6 = 889.964686$ Da. UV–Vis spectroscopic data, taken in CH_3CN ; λ , nm ($\log \epsilon$): 372 (4.61), 472 (4.45), 567 (3.74).

Mn(1DCP3MImP)Cl: MALDI (TOF/TOF): $[\text{M}+\text{H}]^+$: 748.2 Da and HRMS (ESI): 747.10940 Da, in agreement with $\text{MnC}_{38}\text{H}_{26}\text{Cl}_2\text{N}_{10} = 747.109945$ Da. A peak at 1497.2 Da is assigned to a dimer. UV–Vis spectroscopic data taken in $\text{CH}_3\text{CH}_2\text{OH}$: λ , nm ($\log \epsilon$): 370 (4.65), 394 (4.59), 462 (5.06), 559 (4.09), 774 (3.26).

Mn(Porph)-3: MALDI (TOF/TOF): $[\text{M}-2\text{CH}_3]^+$: 762.1 Da corresponding to the loss of 30 Da in relation to the formula $\text{MnC}_{41}\text{H}_{35}\text{Cl}_2\text{N}_{10}$ (792.18 Da). Its HRMS (ESI) showed the molecular peak at 792.16932 Da, according to that formula, and the fragmentation of methyl groups were detected at 777.15260 Da $[\text{M}-\text{CH}_3]^+$ and at 762.12857 Da $[\text{M}-2\text{CH}_3]^+$. However, the spectrum profiles between MALDI and HRMS were different. An intense peak at 919.08125 Da was detected and it could be assigned to $[\text{MnC}_{41}\text{H}_{35}\text{Cl}_2\text{N}_{10}+\text{I}]^+$ (919.08373 Da). UV–Vis spectroscopic data, taken in CH_3CN : λ , nm ($\log \epsilon$): 405 (4.90), 433 (4.71), 562 (4.07) and 592 (*sh.*, 3.82).

Mn(TMImP)Cl: MALDI (TOF/TOF): $[\text{M}]^+ = 683.2$ Da and HRMS (ESI): 683.19349 Da, in agreement with $\text{MnC}_{36}\text{H}_{28}\text{N}_{12} = 683.19$ Da. A peak at 1366.3 Da is assigned to a dimer. UV–Vis spectroscopic data, taken in CH_3CN : λ , nm ($\log \epsilon$): 364 (4.45), 473 (4.50), 579 (3.88).

Mn(Porph)-4: MALDI (TOF/TOF): $[\text{M}-3\text{CH}_3]^+ = 698.2$ Da and HRMS (ESI): 698.21503 Da, corresponding to the loss of 45 Da in relation to the calculated formula $\text{MnC}_{40}\text{H}_{40}\text{N}_{12} = 743.3$ Da. UV–Vis spectroscopic data, taken in CH_3CN : λ , nm ($\log \epsilon$): 396 (4.62), 441 (4.76), 560 (4.09) and 592 (*sh.*, 3.83).

2.3. Catalytic studies

All catalytic studies were carried out in acetonitrile (2.0 mL of total volume). The concentration of the catalyst was 2.5×10^{-4} mol dm $^{-3}$. In the *cis*-cyclooctene oxidation, the substrate/catalyst molar ratio was 600 for catalysts **Mn(Porph)-1**, **Mn(Porph)-3** and **Mn(Porph)-4** and 300 for **Mn(Porph)-2**. For styrene and derivatives catalyzed oxidation, the substrate/catalyst molar ratio was 300 for all catalysts tested. For **Mn(Porph)-1**, ammonium acetate (0.20 mmol) was used as co-catalyst [52,53]. For **Mn(Porph)-4**, acetic acid (0.42 mmol) was chosen as co-catalyst, as it was reported in a recent study [45]. When other co-catalysts are used, that will be mentioned in the text. For the unsymmetric tricationic compound, **Mn(Porph)-3**, the co-catalyst chosen was benzoic acid (0.28 mmol) whereas for the monocationic compound **Mn(Porph)-2**, a buffer system (ammonium acetate/acetic acid – 0.21:0.14 mmol) was used. The oxidant used was 30% (w/w) aqueous H_2O_2 diluted in acetonitrile (1:10) and its addition was made at each 15 min of reaction time, each H_2O_2 addition corresponding to a half-substrate concentration. In temperature-dependent experiments, the same catalytic conditions were used, but changing only the temperature. In Hammett analysis, the temperature was fixed at $25 \pm 2^\circ\text{C}$; the same initial concentration was considered for all olefins to be oxidized. The experiments were run individually. The reactions were followed by GC–FID and GC–MS analysis, using *n*-octane as internal standard. The products identification was made by comparison with the internal GC–MS library.

For *cis*-cyclooctene, the GC run analyses started at 80°C (1 min) increasing at $20^\circ\text{C min}^{-1}$ up to 240°C , keeping this temperature for 2 min (injector and detector at 260°C). For styrenes, the run started at 80°C increasing at $20^\circ\text{C min}^{-1}$ up to 220°C for 6 min (injector at 250°C and detector at 270°C).

2.4. Materials and instrumentation

All solvents and reagents were used as received except pyrrole which was distilled before use and *N,N*-dimethylformamide (DMF) which was dried over activated molecular sieves. Ammonium acetate, acetonitrile and propionic acid were supplied by Merck. Pyrrole, *n*-octane, *cis*-cyclooctene, styrene and 1-methylimidazol-2-carboxaldehyde were purchased from Aldrich. Benzoic acid and H_2O_2 (30% w/w) were purchased from Riedel-de-Häen. Acetic acid was purchased from Panreac. 4-Methylstyrene, 4-chlorostyrene, 4-fluorostyrene, 4-acetoxystyrene and 3-nitrostyrene were purchased from Sigma–Aldrich. 4-Nitrostyrene was received from TCI and nitrobenzene from Acros.

The ^1H and ^{13}C NMR spectra were recorded in a Bruker Avance 300 spectrometer at 300.13 and 75.47 MHz, respectively. CDCl_3 was used as solvent and TMS as the internal reference; chemical shifts are expressed in δ (ppm). The mass spectrometry analyses were carried out in a 4800 MALDI TOF/TOF Analyzer, Applied Biosystems, with and without matrix. The UV/Visible measurements were recorded with a Shimadzu UV-2501 spectrophotometer. The high resolution mass spectrometry (HRMS) analyses were recorded at the University of Vigo, Spain, in a VG Autospec M mass spectrometer using ESI and micro-TOF techniques.

The gas chromatograph (GC) used was a Varian 3900 apparatus equipped with a Chrompack capillary column (CP-Sil 8 CB, $30 \text{ m} \times 0.25 \text{ mm i.d.}; 0.25 \mu\text{m}$ film thickness). The thermostatic bath used in the kinetic studies was purchased from Grant Instruments Ltd.

3. Results and discussion

3.1. Catalytic conditions and mechanistic approach

The catalytic conditions used to perform the epoxidation studies are summarized in Table 1 for *cis*-cyclooctene. The selection of the conditions, namely of the co-catalysts, ammonium acetate for **Mn(Porph)-1** and acetic acid for **Mn(Porph)-4**, was based on our previous results [45,53]. For the new unsymmetrical compounds the optimization studies were carried out with *cis*-cyclooctene; they reflect some co-catalyst dependence on the catalyst structure. The unsymmetrical **Mn(Porph)-2** requires, for a good performance, the presence of ammonium acetate and acetic acid, such as the symmetric porphyrins, **Mn(Porph)-1** and **Mn(Porph)-4**. For **Mn(Porph)-3**, the best efficiency is attained only if an organic acid is present. Benzoic acid is the best co-catalyst for this derivative.

The presence of only one imidazolium-moiety seems to affect significantly the efficiency of this set of porphyrins. **Mn(Porph)-2** was the only one that was unable to provide 100% of conversion, even using a substrate/catalyst ratio lower than for the other catalysts.

Fig. 1 shows the electronic spectra of the unsymmetrical compounds, **Mn(Porph)-2** and **Mn(Porph)-3**, before and after H_2O_2 addition. In the former case, after the oxidant addition, a sharp band at 415 nm appears, and almost all the initial manganese(III) complex, which absorbs at 470 nm, is consumed. In the latter compound only a very small red-shift in the main absorption band from 441 nm to 446 nm is detected.

The absorption band at shorter wavelengths has been reported by Groves [54–56] to be due to an oxidized and inactive catalytic species (Mn(IV) state).

It should be mentioned that during the **Mn(Porph)-1** catalyzed oxidation reactions the observed ratio of $A_{425 \text{ nm}}/A_{475 \text{ nm}}$ is much lower than the one observed with **Mn(Porph)-2**, keeping the catalyst in active form for a longer reaction time. For **Mn(Porph)-2** the

Table 1
cis-Cyclooctene epoxidation with H₂O₂ catalyzed by manganese-porphyrins.^a

Entry	Catalysts	Co-catalyst (mmol)	Reaction time (min)	Substrate/catalyst ratio	Catalyst stability (%)	<i>cis</i> -Cyclooctene epoxide (%)	Reference
1	Mn(Porph)-1	NH ₄ CH ₃ CO ₂ (0.20)	45–60	600	59.7	100	[47]
2	Mn(Porph)-2	CH ₃ COOH/ NH ₄ CH ₃ CO ₂ (0.14:0.21)	90	300	79.8	84	This work
3	Mn(Porph)-3	C ₆ H ₅ COOH (0.28)	75	600	56.7	100	This work
4	Mn(Porph)-4	CH ₃ COOH (0.42)	60–75	600	53.5	100	[45]

^a The oxidant, H₂O₂, was added each 15 min in aliquots corresponding to a half-substrate concentration. Conditions: acetonitrile was used as solvent, at room temperature (25 ± 2 °C). The epoxide yield was always based on the initial substrate amount.

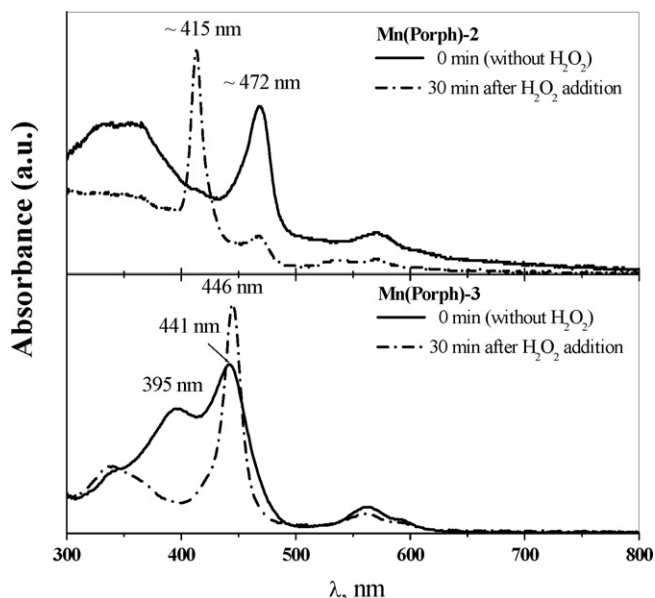
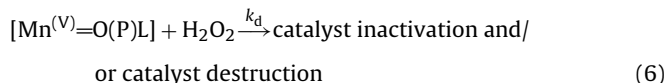
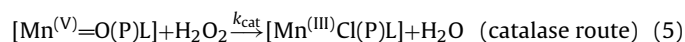
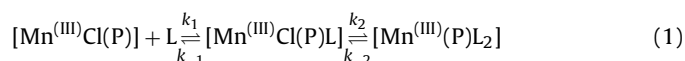


Fig. 1. Electronic spectra in CH₃CN for the unsymmetrical metalloporphyrins before and 30 min after H₂O₂ addition during *cis*-cyclooctene epoxidation.

partial inactivation occurring immediately after the addition of the oxidant might be responsible by its lower performance.

For **Mn(Porph)-3**, the small red-shift detected after the addition of oxidant is similar to the trend detected for the symmetric tetra-substituted imidazolium porphyrin **Mn(Porph)-4** [45].

Eqs. (1)–(6) can then justify the reactions performed here (for details, see [topic S1 in supporting information](#)).



After achieving the equilibrium with the co-catalyst (Eq. (1)), preferably the mono-coordinated species reacts with H₂O₂ producing the hypervalent oxomanganese species (Eq. (2)). The latter can follow different routes: the desired one (*monooxygenase* route), transferring the oxygen to the substrate giving rise to the epoxide (Eq. (4)); the *catalase* route, which favors the H₂O₂ dismutation,

a typical process of cationic manganese porphyrins [16,32] (Eq. (5)) and manganese-containing compounds [57]; and the catalyst inactivation/destruction (Eq. (6)), making it inactive towards oxidation or through destruction of the porphyrin ligand. To avoid or minimize these two undesired processes, the oxidant is loaded fractionally into the system which allowed to apply the steady-state approach (Eq. (4) → Eq. (2)) [58].

Eq. (3) is related to the key step in the *monooxygenase* route [13,27]. Once formed the hyper-oxomanganese species, the [substrate–catalyst][‡] interaction can lead to the desired epoxide as well as to some rearranged products, the latter resulting from radical chain pathways (Scheme 1) [59] or even allylic oxidation products [60,61].

In order to shed some light on the nature of the reactive intermediate involved in epoxidation processes with H₂O₂ in the presence of the imidazolium-based catalysts of Scheme 2A, it was decided to carry out temperature-dependent experiments and Hammett analysis using styrene and styrene derivatives as substrates.

3.2. Thermodynamic analysis

Styrene was catalytically oxidized by the set of metalloporphyrins shown in Scheme 2B using the same styrene/catalyst ratio of 300 in all cases. The experiments were carried out at four temperatures ranging from 3.8 °C to 48 °C. The results obtained for each catalyst are summarized in Table 2.

In the presence of all catalysts the formation of the epoxide (>79%) is the main oxidation pathway. In general, in the presence of the catalysts **Mn(Porph)-1** and **Mn(Porph)-2**, the amount of the epoxide has a slight increase with the increase in temperature. The formation of the by-product, phenylacetaldehyde, was observed under all conditions and usually an increase in the amount of epoxide also brings a decrease in the amount of that by-product. The formation of the radical chain product (*i.e.* benzaldehyde) was also observed but only in trace amounts or as a minor component (<3%).

For Bruce and co-workers [62] the formation of the so-called “rearranged aldehyde” (phenylacetaldehyde) comes from the contribution of a Mn(IV) species formed after the substrate binding (Scheme 1). They also suggest that the charge-transfer complex (such as it is highlighted in Eq. (3)) is the rate-determining step to form the Mn(IV) species but such contribution depends on several factors including the substrate oxidation potential, catalyst symmetry and the propensity of the substrate to undergo rearrangements. Shaik, de Visser and Kumar [39,63] propose that phenylacetaldehyde is originated from cationic/radical type intermediates (Scheme 1, **species III and IV**), in agreement with the proposals from Groves and Myers [64] and others [35,40,65].

Table 2
Temperature-dependence results for styrene oxidation with H₂O₂ catalyzed by manganese porphyrins.^a

Entry	Catalyst	Co-catalyst (mmol)	Temperature, °C (K)	Catalyst stability ^b (%)		Conversion ^c (%)	Product selectivity (%)		
				30 min	60 min		ϕ -CHO	ϕ -CH ₂ CHO	Epoxide
1	Mn(Porph)-1	NH ₄ CH ₃ CO ₂ , 0.20	3.8 (276.95)	100	90	100	1.4 ± 0.6	20.0 ± 4.7	80.0 ± 4.7
2			13.8 (286.95)	95.8	91.9	100	1.7 ± 0.4	16.5 ± 3.8	83.5 ± 3.8
3			25.0 (298.15)	91.3	88.9	100	1.9 ± 0.6	16.9 ± 2.9	80.9 ± 3.1
4			48.0 (321.15)	93.4	89.3	100	2.6 ± 0.8	6.5 ± 3.5	93.5 ± 3.5
5	Mn(Porph)-2	NH ₄ CH ₃ CO ₂ / CH ₃ CO ₂ H 0.21:0.14	3.8 (276.95)	95.9	86.9	87	2.0 ± 0.8	20.6 ± 2.2	79.4 ± 2.2
6			13.8 (286.95)	100	100	96	2.0 ± 0.3	17.6 ± 1.9	82.4 ± 1.9
7			25.0 (298.15)	93.8	72.5	73	2.3 ± 0.1	6.9 ± 3.5	93.1 ± 3.5
8			48.0 (321.15)	76.5	70.6	65	1.6 ± 0.7	8.3 ± 2.3	91.7 ± 2.3
9	Mn(Porph)-3	C ₆ H ₅ CO ₂ H, 0.28	3.8 (276.95)	82.8	84.1	100	<1	17.6 ± 4.5	82.0 ± 4.2
10			13.8 (286.95)	83.5	70.5	100	<1	13.6 ± 4.1	85.9 ± 3.8
11			25.0 (298.15)	72.0	62.7	100	<1	6.4 ± 3.6	93.6 ± 3.6
12			48.0 (321.15)	83.8	76.5	72	<1	19.2 ± 2.5	80.4 ± 2.3
13	Mn(Porph)-4	CH ₃ CO ₂ H, 0.42	3.8 (276.95)	83.7	82.9	100	<1	20.9 ± 4.4	79.1 ± 4.4
14			13.8 (286.95)	95.0	76.3	100	<1	19.2 ± 6.0	80.8 ± 6.0
15			27.0 (300.15)	72.6	56.5	100	<1	18.4 ± 6.7	81.4 ± 6.5
16			45.0 (318.15)	71.0	46.8	70	1.4 ± 1.3	17.6 ± 4.0	82.4 ± 4.0
17	Mn(Porph)-4^d	C ₆ H ₅ CO ₂ H, 0.42	13.8 (286.95)	72.8	66.3	100	<1	16.3 ± 4.0	83.7 ± 4.0
18			27.0 (300.15)	78.5	66.2	100	<1	18.1 ± 6.1	81.9 ± 6.1
19			43.5 (316.65)	72.6	53.9	100	<1	17.9 ± 4.1	82.1 ± 4.1

^a Conditions: catalyst (0.5 μmol), substrate (0.15 mmol), oxidant (H₂O₂ – 0.075 mmol/15 min).

^b Calculated by integrating the absorbance area.

^c At the end of reaction, 90 min. Exceptionally, for **Mn(Porph)-2**, the results are at 120 min of reaction time.

^d The co-catalyst employed was benzoic acid.

To ascertain if under our conditions the phenylacetaldehyde is originated from a radical chain process or by epoxide rearrangement, some experiments were carried out in the presence of BHT, a known radical scavenger. The oxidation of styrene in the presence of **Mn(Porph)-4** was repeated with two different amounts of the radical scavenger: styrene/5 mol% BHT and styrene/50 mol% BHT. In both cases no difference was detected in the epoxide/phenylacetaldehyde ratio, although in the second test the BHT, like styrene, was also consumed (Figure S8, supporting information). This result suggests that phenylacetaldehyde, being formed in all experiments, is not originated by a radical type intermediate.

In order to get more information about this matter, another experiment was carried out. Styrene epoxide (Aldrich, 97% pure) was used as substrate, under the catalytic conditions already established for the oxidation of styrene. The conversion of the epoxide into phenylacetaldehyde was not detected. The epoxide isomerisation is then unlikely in our experimental catalytic conditions (Figure S9, supporting information); this is in agreement with results already reported by others [40,65].

Concerning the catalyst stability, Table 2 shows the stability measured at 30 and 60 min of reaction time, where the [H₂O₂] = [Styrene]₀ and [H₂O₂] = 2 × [Styrene]₀, respectively. It seems that in the presence of the imidazolium-containing manganese porphyrins the lower conversions observed at higher temperatures are due to different factors. This feature is more pronounced for **Mn(Porph)-2**. As shown in Fig. 2A, for this catalyst, a new band arises around 415 nm. The ratio between the new band and the initial band (472 nm) is a good probe to evaluate the catalyst integrity. When the absorbance ratio $A_{415\text{nm}}/A_{472\text{nm}}$ is small (for 3.8 °C and 13.8 °C), higher conversions are observed, whereas when that ratio is high, the substrate conversion decreases (for 25 °C and 48 °C).

On the other hand, for **Mn(Porph)-3** and **Mn(Porph)-4**, the loss of catalytic activity is probably related to catalyst destruction, and not due to their inactivation. Fig. 2B shows the spectral changes for **Mn(Porph)-4** after 30 min of reaction time at the considered temperature values. Unlike what happens with **Mn(Porph)-2**,

the tetracationic compound undergoes destruction, mainly after 60 min (Table 2). Also, the electronic spectral profile at 3.8 °C and 13.8 °C resembles the initial spectrum ($t = 0$ min) and at 27 °C and 45 °C, the sharp band at 446 nm becomes predominant, although being followed by reduction in its intensity.

Following the styrene consumption by GC analysis, the rate constant (k_{obs} , in min⁻¹) could be evaluated using the proposed mechanism (as shown in Eqs. (1)–(6); for details, see topic S1 in supporting information). Manipulating the data into the Eyring Transition State theory (Eq. (7)), we were able to estimate the activation thermodynamic parameters (Table 3) for styrene oxidation reactions (Table S1 and Figs. S3–S7 in supporting information).

$$\ln\left(\frac{k_{\text{obs}}}{T}\right) = \ln\left(\frac{k_{\text{B}}}{h}\right) + \frac{\Delta S^{\ddagger}}{R} - \frac{\Delta H^{\ddagger}}{R \cdot T} \quad (7)$$

where k_{obs} is the pseudo-zero order rate constant, k_{B} is the Boltzmann constant, h is Planck's constant, R is the ideal gas constant and T the temperature, in Kelvin.

The results summarized in Table 3 show that, under the used catalytic conditions, the Gibbs activation energy (ΔG^{\ddagger}) values are very close to each other; however, catalyst **Mn(Porph)-1** presents the lower free energy barrier (80.3 kJ mol⁻¹). The activation parameters found show that the pair **Mn(Porph)-3** and **Mn(Porph)-4** exhibit an enthalpy–entropy compensation with isokinetic temperature equals to 29.9 °C (within the studied temperature range). Also, the pair **Mn(Porph)-1** and **Mn(Porph)-2** follow a similar behavior, however, the isokinetic temperature is out of the studied temperature range (in this case, around –7.54 °C, by extrapolation), such as it is described in the literature [66] and in studies involving ligand [67] and substrate binding [68] to cytochrome P450 mutants. For the symmetric catalyst, **Mn(Porph)-4**, the activation enthalpy is exothermic, even when the co-catalyst was changed from acetic to benzoic acid (Table 3, entries 4 and 5), such as observed for **Mn(Porph)-3**. The effect of the co-catalyst in the reactions performed with **Mn(Porph)-4** is related to the catalyst integrity, allowing full substrate conversion even at higher temperatures; this was not observed when acetic acid was used (Table 2, entries 16 and 19, for acetic and benzoic acids, respectively).

Table 3
Activation parameters for styrene oxidation with H₂O₂ catalyzed by manganese porphyrins.

Entry	Catalyst	ΔS^\ddagger (JK ⁻¹ mol ⁻¹)	$-T \cdot \Delta S^\ddagger$ (kJ mol ⁻¹)	ΔH^\ddagger (kJ mol ⁻¹)	ΔG^\ddagger (kJ mol ⁻¹)
1	Mn(Porph)-1	-158.0	47.1	33.2	80.3
2	Mn(Porph)-2	-260.4	77.6	5.3	82.9
3	Mn(Porph)-3	-390.3	116.4	-33.8	82.6
4	Mn(Porph)-4^b	-323.2	96.4	-14.7	81.7
5	Mn(Porph)-4^c	-323.6	96.5	-15.6	81.0

^a At 298 K.

^b With acetic acid (0.42 mmol) as co-catalyst.

^c With benzoic acid (0.42 mmol) as co-catalyst.

Such results show that, under those conditions, styrene oxidation is an enthalpy-controlled reaction when catalyzed by **Mn(Porph)-1** or by **Mn(Porph)-2** whereas it is entropy-controlled when catalyzed by **Mn(Porph)-3** or **Mn(Porph)-4** (Fig. 3).

Thus, an explanation [69] for the observed exothermic activation enthalpy is that the reaction involves the initial exothermic formation of a substrate–catalyst complex which can undergo a competitive collapse either to starting material or to product(s); the free energy barrier for product formation must have an enthalpy value lower than that for the complex reverse. Moreover, for a negative activation enthalpy, the substrate–catalyst

complex must be well organized resulting in a strong entropic term. Usually, under these circumstances, the reaction rate must decrease when the temperature increases as it was verified with our catalysts **Mn(Porph)-3** and **Mn(Porph)-4** (Figs. S5 and S6 in supporting information).

The negative activation enthalpy observed for catalysts **Mn(Porph)-3** and **Mn(Porph)-4** can be attributed to the best solvation effect caused by the CH₃CN (solvent) and the water (by-product from H₂O₂), thus leading the high-valent catalyst species to a lower energy plateau followed by a best organized cage (favoring a lower entropy, as observed). This is expected since those catalysts possess three and four cationic centres (Scheme 2B).

After that the substrate binding is exothermic as well, further decreasing the relative energy. The energy barrier for the oxygen transfer process into the substrate must not be too high to originate an overall positive activation enthalpy. Although it can be merely speculative, such hypothesis coincides with some features observed by Curet-Arana et al. [70] in an assisted computational work involving a manganese porphyrin model in olefins' epoxidation, and by Khenkin et al. in a work involving oxidation studies with a Mn-polyoxometalate as catalyst [71]. Those authors used DFT calculation and spin crossing effects to explain the observed activation parameters in the reactions studied. In the same fashion, Groves et al. studied the isomeric oxo-manganese(V) complexes of 2- and 4-methylpyridinium porphyrins ([Mn(V)=O(2TMPyP)] and [Mn(V)=O(4TMPyP)]), respectively and observed reactivity differences between these two isomers, which were attributed to spin crossing effects [72]. By analogy, the same author studied the **Mn(Porph)-4**, showing that at lower pH, the spin crossing effect become predominant, thus facilitating the oxygen transfer process

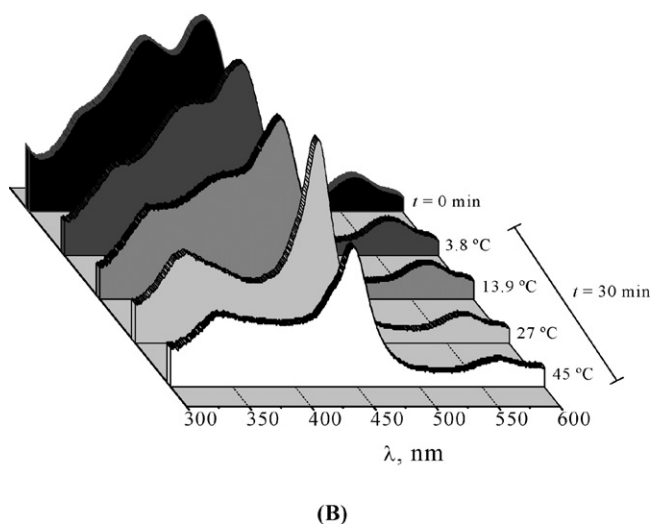
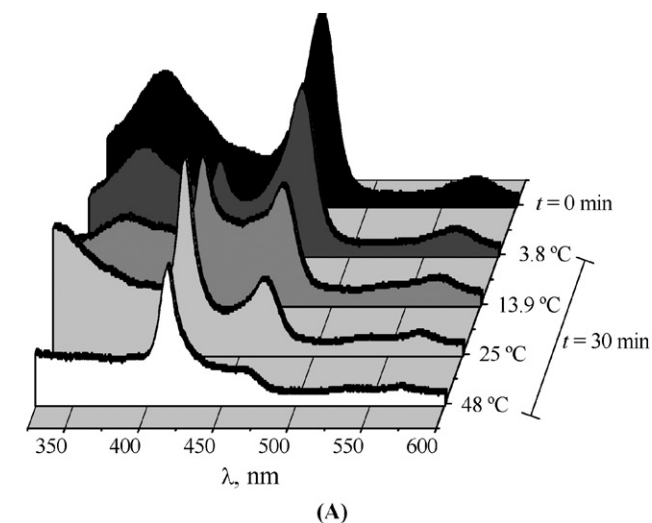


Fig. 2. Spectral changes after 30 min of reaction at each temperature considered for catalysts (A) **Mn(Porph)-2** and (B) **Mn(Porph)-4**.

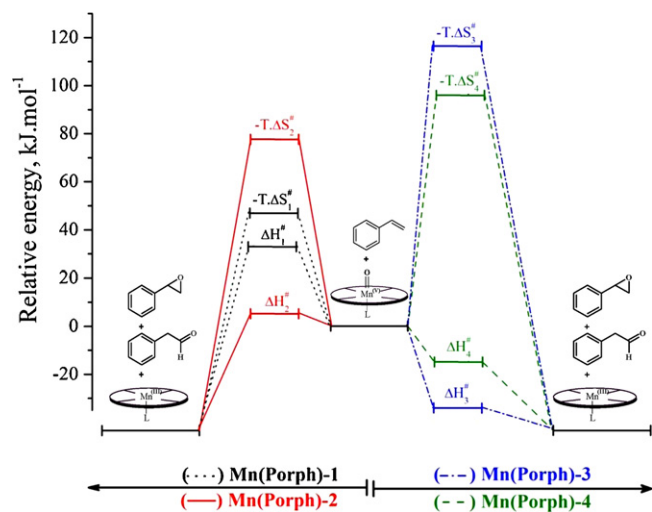


Fig. 3. Energetic view profile for styrene oxidation with H₂O₂ catalyzed by the manganese-porphyrins shown in Scheme 2B. The ΔG^\ddagger is shown as a function of $-T \cdot \Delta S^\ddagger$ ($\Delta G^\ddagger = \Delta H^\ddagger - T \cdot \Delta S^\ddagger$) for $T=298.15$ K. The maximum error found in those measurements was 10%.

[73]. That effect was also postulated for other metalloporphyrins rather than the manganese complexes [28,54,71–76].

Regarding to the activation parameters observed for **Mn(Porph)-1** and **Mn(Porph)-2**, the former is the most important example of metalloporphyrin based catalysts for alkane and alkene oxygenation and the values reported for that derivative are in agreement with studies reported by Nam et al. [77]. Among these two catalysts, the activation enthalpy observed for **Mn(Porph)-2** catalyzed reactions is lower than that for **Mn(Porph)-1**, showing a disturbing effect of imidazolium moiety on the catalyst structure although the ΔS^\ddagger and ΔH^\ddagger values for **Mn(Porph)-1** and **Mn(Porph)-2** show the same trend found for other oxidation studies employing metalloporphyrins as catalysts [29,78].

The imidazolium portion attached to the porphyrin macrocycle seems to disturb the electronic distribution, affecting the thermodynamic activation parameters on styrene catalyzed oxidation. When the imidazolium portion increases on the catalyst, the activation enthalpy decreases (Table 3). The trend is affected when the data between **Mn(Porph)-3** and **Mn(Porph)-4** are compared (Table 3, entries 3–5). The differences between these catalysts could be attributed to the symmetry differences (C_{2v} for **Mn(Porph)-3** and D_{4h} for **Mn(Porph)-4**).

3.3. Hammett studies

In order to complement the previous studies, the oxidation of several phenyl-substituted styrenes was performed at room temperature ($25 \pm 2^\circ\text{C}$) in the presence of the same series of catalysts. The results presented in Table 4 summarize the substrate conversion and the products selectivity for each styrene derivative.

From the experiments using styrene derivatives and plotting the data in Hammett Equation (Eq. (8)) [79,80], a typical Hammett correlation (ρ) is obtained.

$$\log \frac{k_X}{k_H} = \rho\sigma^* \quad (8)$$

Fig. 4 shows the typical Hammett plot for the best correlation found for each catalyst using some selected substrates from Table 4.

In all our results, the epoxide/phenylacetaldehyde ratio underwent variation according to the substituent attached in styrene; however, the substrate consumption rate is almost independent of the substituent effect (Table S2 in supporting information). It is worth to note that the influence of the porphyrin structure on the selectivity; in the oxidation reactions catalyzed by the symmetric **Mn(Porph)-1** and **Mn(Porph)-4** derivatives, similar epoxide/phenylacetaldehyde ratio was observed for all substrates tested. The unsymmetrical derivatives **Mn(Porph)-2** and **Mn(Porph)-3** exhibited, in general, high selectivity towards epoxide (Table S3 in supporting information).

The ρ -values obtained using the Hammett equation for the oxidation of styrene and derivatives in the presence of the studied metalloporphyrins are in good agreement with some values already described in the literature [29,62,81]. The values reported here, between -0.15 and -0.61 , indicate that there is no significant charge separation in the transition state, suggesting that cationic intermediates can be formed only in a small percentage during the oxidation process.

A ρ -value near zero could indicate a multi-step mechanism in which the rate determining step does not involve the substrate binding. Excluding the nitrostyrene derivatives, the other set of olefins exhibited rates very close to each other, suggesting that the substrate binding is not the determining step in the reactions involving those substrates (Figs. S10–S13 and Table S2 in supporting information).

A similar behavior was observed by Campestrini and Cagnina [82] in the oxidation reactions of 1-phenylethanol derivatives

with tetraphenylphosphonium monopersulfate catalyzed by two manganese porphyrins. The authors observed that the Hammett analysis was dependent on the employed experimental technique (individual or competitive reactions) [82].

Commonly, a concerted mechanism is invoked to explain the small ρ -value. However, effects of multi-step reaction in which the overall ρ -values of all steps cancel each other [83–85] can be considered as well as the ligand stabilizing effect.

Regarding the multi-step reaction, Hammett studies involving ruthenium-porphyrins in substituted-styrenes catalyzed oxidation showed that the transition states differ when the substituents are $-\text{CH}_3$, $-\text{H}$, $-\text{Cl}$ and $-\text{OCH}_3$. In the former, a concerted mechanism is expected while in the latter, a cationic intermediate is thought to explain the amount of phenylacetaldehyde observed [86]. The ligand stabilizing effect was demonstrated for iron-porphyrins [87,88] and it is more pronounced in manganese analogues since in such cases a ligand is required to perform and to stabilize the generated electrophilic oxidant [82,89,90]. Nevertheless, the ligand effect was not pronounced for **Mn(Porph)-4** catalyzed reactions as observed in the unsubstituted styrene as shown in Table 2 (entries 14–17) when the co-catalyst was changed from acetic to benzoic acid.

The products' distribution cannot be rationalized based on the inductive effects (electron-withdrawing or electron-donating effects) caused by substituents, as used in the conventional Hammett theory. For example, for *m*- and *p*-nitrostyrene oxidation, only the epoxide was produced as expected for an "oxene" type oxygen transfer, whereas for *p*-methylstyrene a considerable yield of corresponding phenylacetaldehyde was obtained (Table 4). The *p*-fluorostyrene and *p*-chlorostyrene showed similar epoxide/phenylacetaldehyde ratio when compared to the unsubstituted styrene in the oxidation catalyzed by the symmetric catalysts. In those cases, the inductive electron-withdrawing character of such substituents is lower than their resonance effects. The oxidation of *p*-acetoxystyrene shows different behaviors depending on the catalyst structure; IUPAC recommends caution in using the Hammett values with that substituent [80]. The behavior of *p*-acetoxystyrene showed, in some cases, a resonance effect higher than its inductive effect. For the symmetric catalysts, the oxidation of this styrene derivative gave the epoxide/phenylacetaldehyde very close to the poor induced electron-donating *p*-methylstyrene (Table S3 in supporting information).

A hypothetical intermediate was already reported for iron-porphyrin catalyzed reactions to explain the intermediate ring-closure step, generating the epoxide, or the rearrangement step, providing the phenylacetaldehyde [64]. Such observation implies that the product release is strongly influenced by substituents, being the product distribution a substituent-controlled step.

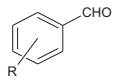
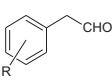
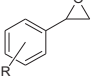
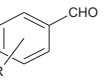
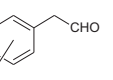
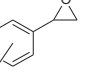
The ^1H and ^{13}C NMR spectra of the studied styrene derivatives were recorded with the purpose of understanding the substituent effect on the vinylic reactivity. When compared with the unsubstituted styrene, no pronounced chemical shifts are observed in the α - and β -signals of the carbons and protons of the derivatives (see Table S3 in supporting information).

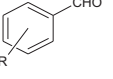
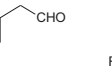
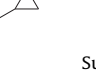
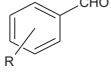
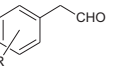
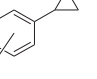
It seems that, once formed the complex between the activated catalyst and the olefin, the vinylic double bond shall be broken and, only after that, the substituent effect will drive the product selectivity. In fact, a mixture of effects (resonance and inductive effects) caused by the substituents will influence the epoxide ring-closure and the formation of the corresponding phenylacetaldehyde.

According to the results obtained here, a correlation between our findings with the intermediates presented in Scheme 1 can be drafted. Some assumptions must be underlined:

- (i) For Mn-porphyrins catalyzed oxidations, it is postulated that (Porph)Mn(V)=O species is the responsible for oxygen transfer with a high rate constant, while (Porph)Mn(IV)=O

Table 4Styrene and its derivatives catalyzed oxidation performed by the studied manganese porphyrins using H₂O₂ as oxidant.

X-Styrene	Catalyst								
	Mn(Porph)-1 ^a			Mn(Porph)-2 ^{b,e}					
									
	Substrate conversion (%)				Substrate conversion (%)				
<i>p</i> -Me	100	2.9 ± 0.8	41.2 ± 10.6	57.4 ± 10.4	85.7	2.8 ± 0.1	21.8 ± 4.8	78.2 ± 4.8	
H	100	1.9 ± 0.6	16.9 ± 2.9	80.9 ± 3.1	82.8	2.3 ± 0.1	6.9 ± 3.5	93.1 ± 3.5	
<i>p</i> -F	100	2.4 ± 0.4	19.5 ± 6.9	80.5 ± 6.9	88.4	2.4 ± 0.2	16.9 ± 2.8	83.1 ± 2.8	
<i>p</i> -Cl	99	1.4 ± 0.7	16.9 ± 4.1	83.1 ± 4.1	83.0	2.0 ± 0.3	15.2 ± 5.8	84.8 ± 5.8	
<i>p</i> -AcO	100	2.2 ± 0.6	44.7 ± 9.7	55.3 ± 9.7	96.1	1.1 ± 0.6	26.2 ± 7.1	73.8 ± 7.1	
<i>m</i> -NO ₂ ^e	100	<1	<1	99.9 ± 0.2	35.8	<1	1.5 ± 1.0	98.5 ± 1.0	
<i>p</i> -NO ₂ ^e	100	0	0	100	77.0	0	0	100	

X-Styrene	Catalyst								
	Mn(Porph)-3 ^c			Mn(Porph)-4 ^d					
									
	Substrate conversion (%)				Substrate conversion (%)				
<i>p</i> -Me	100	<1	16.9 ± 3.7	83.1 ± 3.7		<1	47.4 ± 10.3	52.5 ± 10.2	
H	100	<1	6.4 ± 3.6	93.6 ± 3.6	100	<1	18.4 ± 6.7	81.4 ± 6.5	
<i>p</i> -F	100	<1	21.1 ± 3.1	78.9 ± 3.1	100	<1	24.6 ± 5.8	75.0 ± 5.6	
<i>p</i> -Cl	100	<1	11.7 ± 4.4	88.3 ± 4.4	100	<1	25.8 ± 9.1	74.2 ± 9.1	
<i>p</i> -AcO	100	1.4 ± 0.8	24.0 ± 6.3	76.0 ± 6.3	100	0	47.4 ± 7.7	52.6 ± 7.7	
<i>m</i> -NO ₂ ^e	100	<1	<1	99.1 ± 0.9	61.9	1.4 ± 0.1	<1	98.0 ± 0.2	
<i>p</i> -NO ₂ ^e	97.4	0	0	100	81.0	0	0	100	

Conditions: Reaction volume 2.0 mL, catalyst (0.5 × 10⁻⁶ mol), substrate (0.15 × 10⁻³ mol) and H₂O₂ (0.075 × 10⁻³ mol/15 min). All the reactions were performed under normal atmosphere and T = 25 °C (±2.5 °C).

^a Co-catalyst: NH₄CH₃CO₂ (0.20 mmol).

^b Co-catalyst: NH₄CH₃CO₂ (0.21 mmol) + CH₃COOH (0.14 mmol).

^c Co-catalyst: C₆H₅COOH (0.28 mmol).

^d Co-catalyst: CH₃COOH (0.42 mmol).

^e Epoxidation performed up to 120 min.

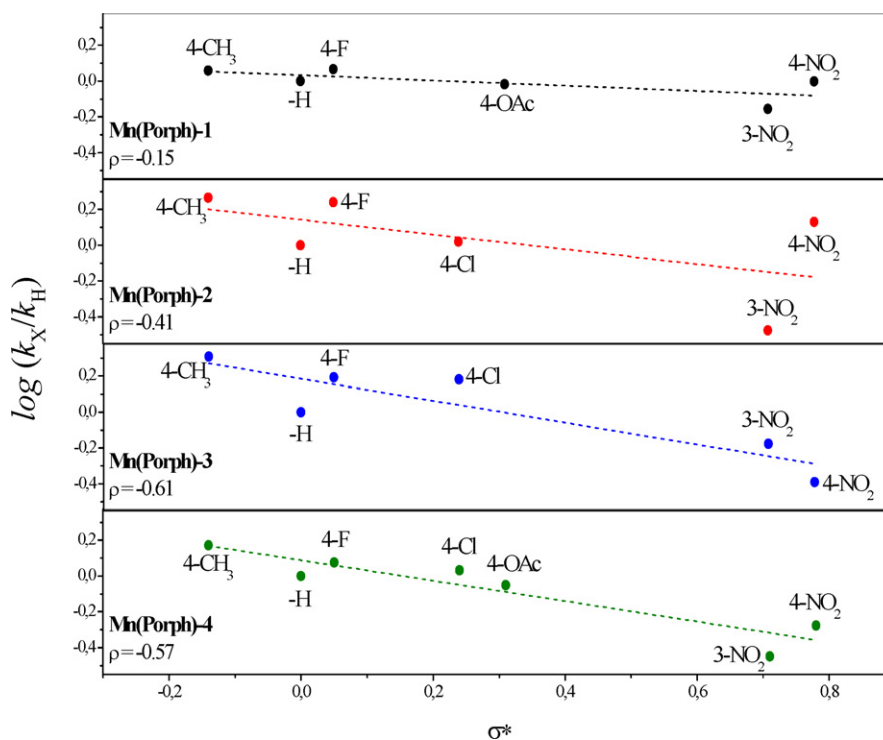


Fig. 4. Hammett plots for styrene derivatives catalyzed oxidation in the presence of manganese porphyrins and H₂O₂.

slowly oxidize alkenes (giving epoxide in low yield) and the [(Porph)Mn(IV)=O]⁺ species can participate in one- and two-electron oxidation reactions [28,62]. The involvement of radical-type intermediates is unlikely for all the catalysts studied. Such intermediate would generate higher amount of benzaldehyde but the results showed in Table 2 do not support that idea. The existence of charged intermediates is disregarded, at least for the imidazolium-containing catalysts. The cationic species should be dependent on the substituent effect in substrate binding step but it is not observed in the reactions studied here under our conditions. To reinforce such hypothesis, the ΔS^\ddagger estimated for imidazolium-containing catalysts is too negative to support the existence of such intermediate. Also, the ρ -values obtained are too small to indicate a great charge separation in the transition state. Furthermore, the experiments using BHT did not show any difference in products distribution. Hence, species (II) to (IV) do not fit well with our results.

- (ii) The metallooxetane species (I) and oxene insertion species (V) are presented as reasonable models to be thought as intermediates in the epoxidation reactions. However, the oxene insertion should give only the corresponding epoxide as in the classical oxidations performed by peracids [85]. The epoxide was produced exclusively when nitrostyrenes were used as substrates. This argument is also confirmed by our experimental results for phenyloxirane oxidation catalyzed by Mn(Porph)-4, showing no production of phenylacetaldehyde; thus, we believe that this aldehyde is originated from the same intermediate of the epoxide and not from its rearrangement. Due to these reasons, species (V) could not be applied as the model intermediate.
- (iii) Finally, the metallo-oxetane species (I) presents suitable features to match the results obtained here. Although a four-membered cycle is too tight to be stable, by other hand, this intermediate is highly organized, supporting the obtained ΔS^\ddagger values. Mechanistically, a multi-step reaction can be thought as in enzymatic systems. In this way, a first approach between substrate and the oxidized metalloporphyrin is given by an oxene-type followed by the metalloxetane formation. In both cases, the reaction is exothermic, as proposed for propene oxidation catalyzed by Mn-porphyrins [70] and in good agreement with the small ΔH^\ddagger reported in Table 3. Thus, the formation of the metalloxetane justifies the phenylacetaldehyde by 1,2-hydride rearrangement in the transition state.

The hypothesis of the metalloxetane as intermediate was discussed in a reference work using metallocompounds in oxidation reactions catalyzed by rhenium and osmium and this idea is reinforced when the oxidant used is H₂O₂ [91]. An excellent review highlights metalloxetanes already reported in the literature and the possibility of their existence in biological and biomimetic processes involving metalloporphyrins [92].

Computational studies on the epoxidation reactions catalyzed by manganese porphyrins showed that metalloxetane species can be assumed as the model intermediate on styrene epoxidation, but with a specific configuration [70]. A recent work described by Curet-Arana et al. [93] has shown the reaction pathway on styrene oxidation catalyzed by a manganese porphyrin and the result found is in excellent agreement with our thermodynamic findings and the hypothesis of singlet–triplet–quintet spin crossing reported by Khenkin et al. [71] and DeAngelis et al. [72].

4. Conclusions

Here we report the catalytic properties of symmetrical and unsymmetrical imidazolium-containing manganese porphyrins

and the results are compared with that obtained with the well established Mn(Porph)-1. Under steady-state conditions, it is possible to show how the thermodynamic activation parameters are affected due to structural differences of the catalyst. The structural differences also change the products selectivity.

The effects upon the activation parameters are followed by a compensation phenomenon where that feature is more favored with the pair Mn(Porph)-3 and Mn(Porph)-4. It should be highlighted that the compensation effect was observed in all cases being the activated Gibbs free energy almost the same. The Hammett analysis provided small ρ -values indicating that there is no significant charge separation in the transition state; this fact is in good agreement with some values already reported in the literature. However, this analysis shows that the substrate binding process is not the determining step and that the product release is strongly influenced by the substituent (inductive and resonance effects) on styrene derivatives. Among the possible intermediates, the results, under the conditions used here, fit well with a proposed concerted reaction pathway, starting from an oxene-type approach followed by a [$\pi 2_a + \pi 2_s$] metallooxetane intermediate, the latter being the determining step. It is worth to mention that different experimental conditions can affect the results, opening the possibility to the involvement of other hypervalent species, resulting in different reaction pathways. In our study, Mn(Porph)-1 presents an activation entropy higher than the other catalysts, but a ρ -value too small to indicate the presence of charged intermediates. Finally, this work provides an insight into the mechanistic pathway towards olefin epoxidation and the effect of the catalysts' ligand and symmetry on the thermodynamic and selectivity reaction features, when hydrogen peroxide is used as oxidant.

Acknowledgements

Thanks are due to Fundação para a Ciência e a Tecnologia (FCT/FEDER) for funding the University of Aveiro Organic Chemistry Research Unit. Authors would like to thank Professor Artur Silva for the useful discussion in NMR analysis, Dr. Fernando Domingues for the apparatus used for kinetic studies, Dr. M. Rosário Domingues for the valuable discussions in mass spectroscopy analysis and Mr. Antonio Morais (Glassblower) for the “tailor-made” thermostatic cell and other glassware used in this study. R. De Paula also thanks FCT for his Ph.D. Grant (SFRH/BD/25666/2005).

Appendix A. Supplementary data

Supplementary data associated with this article can be found, in the online version, at doi:10.1016/j.molcata.2011.05.013.

References

- [1] S. Bhaduri, D. Mukesh, *Homogeneous Catalysis: Mechanisms and Industrial Applications*, Wiley Interscience, New York, 2000.
- [2] H.A. Wittcoff, B.G. Reuben, J.S. Plotkin, *Industrial Organic Chemicals*, second ed., Wiley-Interscience, New Jersey, 2004.
- [3] E. Brulé, Y.R. Miguel, *Org. Biomol. Chem.* 4 (2006) 599–609.
- [4] K.A. Joergensen, *Chem. Rev.* 89 (1989) 431–458.
- [5] D. Mansuy, *C.R. Chim.* 10 (2007) 392–413.
- [6] K. Korzekwa, W. Trager, M. Gouterman, D. Spangler, G. Loew, *J. Am. Chem. Soc.* 107 (1985) 4273–4279.
- [7] F.P. Guengerich, *J. Biol. Chem.* 266 (1991) 10019–10022.
- [8] C.A. Martinez, J.D. Stewart, *Curr. Org. Chem.* 4 (2000) 263–282.
- [9] B. Meunier, S.P. de Visser, S. Shaik, *Chem. Rev.* 104 (2004) 3947–3980.
- [10] I.G. Denisov, T.M. Makris, S.G. Sligar, I. Schlichting, *Chem. Rev.* 105 (2005) 2253–2278.
- [11] F.P. Guengerich, *J. Biochem. Mol. Toxicol.* 21 (2007) 163–168.
- [12] R. Wang, S.P. de Visser, *J. Inorg. Biochem.* 101 (2007) 1464–1472.
- [13] F. Montanari, L. Casella, *Metalloporphyrins Catalyzed Oxidations*, Kluwer Academic Publishers, Dordrecht, 1994.
- [14] R.A. Sheldon, *Metalloporphyrins in Catalytic Oxidations*, Marcel Dekker, Inc., New York, 1994.

- [15] B. Meunier, *Biomimetic Oxidations Catalyzed by Transition Metal Complexes*, Imperial College Press, London, 1999.
- [16] J.E. Backvall, *Modern Oxidation Methods*, Wiley-VCH, Weinheim, 2004.
- [17] W.R. Sanderson, *Pure Appl. Chem.* 72 (2000) 1289–1304.
- [18] M. Ghiasi, M. Tafazzoli, N. Safari, *J. Mol. Struct. (Theochem.)* 820 (2007) 18–25.
- [19] T. Kamachi, T. Kouno, W. Nam, K. Yoshizawa, *J. Inorg. Biochem.* 100 (2006) 751–754.
- [20] S.P. de Visser, *J. Biol. Inorg. Chem.* 11 (2006) 168–178.
- [21] S. Jin, T.M. Makris, T.A. Bryson, S.G. Sligar, J.H. Dawson, *J. Am. Chem. Soc.* 125 (2003) 3406–3407.
- [22] F. Montanari, S. Banfi, S. Quici, *Pure Appl. Chem.* 61 (1989) 1631–1636.
- [23] F. Montanari, *Pure Appl. Chem.* 66 (1994) 1519–1526.
- [24] A.M.A.R. Gonsalves, M.M. Pereira, *J. Mol. Catal. A: Chem.* 113 (1996) 209–221.
- [25] R. Noyori, M. Aoki, K. Sato, *Chem. Commun.* (2003) 1977–1986.
- [26] D. Rutkowska-Zbik, M. Witko, *J. Mol. Catal. A: Chem.* 258 (2006) 376–380.
- [27] B. Meunier, A. Robert, G. Pratiel, J. Bernadou, in: K.M. Kadish, K.M. Smith, R. Guilard (Eds.), *The Porphyrin Handbook*, Academic Press, 2000, p. 119.
- [28] S. Banfi, M. Cavazzini, G. Pozzi, S.V. Barkanova, O.L. Kaliya, *J. Chem. Soc. Perkin Trans. 2* (2000) 871–877.
- [29] L. Zeng, H.J.H. Wang, A. Lei, J.I. Brauman, J.P. Collman, *Eur. J. Org. Chem.* 2006 (2006) 2707–2714.
- [30] A.C. Serra, E.C. Marçalo, A.M.A.R. Gonsalves, *J. Mol. Catal. A: Chem.* 215 (2004) 17–21.
- [31] H. Turk, M. Erdem, *J. Porphyrins Phthalocyanines* 8 (2004) 1196–1203.
- [32] R. Belal, M. Momenteau, B. Meunier, *J. Chem. Soc. Chem. Commun.* (1989) 412–414.
- [33] S.P. deVisser, *Inorg. Chem.* 45 (2006) 9551–9557.
- [34] N.A. Stephenson, A.T. Bell, *J. Mol. Catal. A: Chem.* 272 (2007) 108–117.
- [35] A.A. Guedes, A. Santos, M.D. Assis, *Kinet. Catal.* 47 (2006) 555–563.
- [36] M.D. Assis, A.O.J.B. Melo, P.B. Pereira, O.A. Serra, Y. Iamamoto, M. Moraes, *J. Inorg. Biochem.* 51 (1993) 263–292.
- [37] Y. Iamamoto, M.D. Assis, K.J. Ciuffi, C.M.C. Prado, B.Z. Prellwitz, M. Moraes, O.R. Nascimento, H.C. Sacco, *J. Mol. Catal. A: Chem.* 116 (1997) 365–374.
- [38] S.S. Kurek, P. Michorczyk, A.M. Balisz, *J. Mol. Catal. A: Chem.* 194 (2003) 237–248.
- [39] D. Kumar, S.P. de Visser, S. Shaik, *Chem. Eur. J.* 11 (2005) 2825–2835.
- [40] Y. Liu, H.J. Zhang, Y. Lu, Y.Q. Cai, X.L. Liu, *Green Chem.* 9 (2007) 1114–1119.
- [41] M. Fontecave, D. Mansuy, *J. Chem. Soc. Chem. Commun.* (1984) 879–881.
- [42] A.M.A.R. Gonsalves, A.C. Serra, *J. Chem. Soc. Perkin Trans. 2* (2002) 715–719.
- [43] J.P. Collman, T. Kodadek, J.I. Brauman, *J. Am. Chem. Soc.* 108 (1986) 2588–2594.
- [44] Y. Miyazaki, A. Satake, Y. Kobuke, *J. Mol. Catal. A: Chem.* 283 (2008) 129–139.
- [45] R. De Paula, M.M.Q. Simões, M.G.P.M.S. Neves, J.A.S. Cavaleiro, *Catal. Commun.* 10 (2008) 57–60.
- [46] R. De Paula, M.A.F. Faustino, D.C.G.A. Pinto, M.G.P.M.S. Neves, J.A.S. Cavaleiro, *J. Heterocycl. Chem.* 45 (2008) 453–459.
- [47] A.M.A.R. Gonsalves, J.M.T.B. Varejao, M.M. Pereira, *J. Heterocycl. Chem.* 28 (1991) 635–640.
- [48] J.P.C. Tomé, M.G.P.M.S. Neves, A.C. Tomé, J.A.S. Cavaleiro, M. Soncin, M. Magaraggia, S. Ferro, G. Jori, *J. Med. Chem.* 47 (2004) 6649–6652.
- [49] A.M.A.R. Gonsalves, M.M. Pereira, A.C. Serra, R.A.W. Johnstone, M.L.P.G. Nunes, *J. Chem. Soc. Perkin Trans. 1* (1994) 2053–2057.
- [50] D.H. Tjahjono, T. Akutsu, N. Yoshioka, H. Inoue, *Biochim. Biophys. Acta (BBA): Gen. Subjects* 1472 (1999) 333–343.
- [51] J.D. Crapo, B.J. Day, M.P. Trova, P.J.F. Gauuan, D.B. Kitchen, I. Fridovich, I. Batinic-Haberle, in: U.S. Patent (Ed.), *Substituted Porphyrins*, National Jewish Medical and Research Center, Aeolus Pharmaceuticals Inc., Duke University, USA, 2003, pp. 1–39.
- [52] S.L.H. Rebelo, *Metaloporfirinas: síntese e oxidação catalítica de compostos orgânicos com peróxido de hidrogénio*, Departamento de Química, Universidade de Aveiro, Aveiro/Portugal, 2003.
- [53] S.L.H. Rebelo, M.M. Pereira, M.M.Q. Simões, M.G.P.M.S. Neves, J.A.S. Cavaleiro, *J. Catal.* 234 (2005) 76–87.
- [54] J.T. Groves, W.J. Kruper, R.C. Haushalter, *J. Am. Chem. Soc.* 102 (1980) 6375–6377.
- [55] J.T. Groves, M.K. Stern, *J. Am. Chem. Soc.* 109 (1987) 3812–3814.
- [56] J.T. Groves, M.K. Stern, *J. Am. Chem. Soc.* 110 (1988) 8628–8638.
- [57] Y.G. Abashkin, S.K. Burt, *Inorg. Chem.* 44 (2005) 1425–1432.
- [58] K.J. Laidler, *Pure Appl. Chem.* 68 (1996) 149–192.
- [59] A.A. Shteinman, *Russ. Chem. Bull.* 50 (2001) 1795–1810.
- [60] S.-E. Park, W.J. Song, Y.O. Ryu, M.H. Lim, R. Song, K.M. Kim, W. Nam, *J. Inorg. Biochem.* 99 (2005) 424–431.
- [61] A. Agarwala, D. Bandyopadhyay, *Catal. Lett.* 124 (2008) 256–261.
- [62] R.D. Arasasingham, G.X. He, T.C. Bruce, *J. Am. Chem. Soc.* 115 (1993) 7985–7991.
- [63] S.P. de Visser, D. Kumar, S. Shaik, *J. Inorg. Biochem.* 98 (2004) 1183–1193.
- [64] J.T. Groves, R.S. Myers, *J. Am. Chem. Soc.* 105 (1983) 5791–5796.
- [65] Y. Liu, H.J. Zhang, Y.Q. Cai, H.H. Wu, X.L. Liu, Y. Lu, *Chem. Lett.* 36 (2007) 848–849.
- [66] G.C. Bond, M.A. Keane, H. Kral, J.A. Lercher, *Catal. Rev.* 42 (2000) 323–383.
- [67] B.K. Muralidhara, S.S. Negi, J.R. Halpert, *J. Am. Chem. Soc.* 129 (2007) 2015–2024.
- [68] B.K. Muralidhara, L. Sun, S. Negi, J.R. Halpert, *J. Mol. Biol.* 377 (2008) 232–245.
- [69] C.J. Bradaric, W.J. Leigh, *J. Am. Chem. Soc.* 118 (1996) 8971–8972.
- [70] M.C. Curet-Arana, G.A. Emberger, L.J. Broadbelt, R.Q. Snurr, *J. Mol. Catal. A: Chem.* 285 (2008) 120–127.
- [71] A.M. Khenkin, D. Kumar, S. Shaik, R. Neumann, *J. Am. Chem. Soc.* 128 (2006) 15451–15460.
- [72] F. DeAngelis, N. Jin, R. Car, J.T. Groves, *Inorg. Chem.* 45 (2006) 4268–4276.
- [73] D. Lahaye, J.T. Groves, *J. Inorg. Biochem.* 101 (2007) 1786–1797.
- [74] N. Jin, M. Ibrahim, T.G. Spiro, J.T. Groves, *J. Am. Chem. Soc.* 129 (2007) 12416–12417.
- [75] J.T. Groves, W.J. Kruper, *J. Am. Chem. Soc.* 101 (1979) 7613–7615.
- [76] N. Jin, J.T. Groves, *J. Am. Chem. Soc.* 121 (1999) 2923–2924.
- [77] W.J. Song, M.S. Seo, S. DeBeer George, T. Ohta, R. Song, M.J. Kang, T. Toshi, T. Kitagawa, E.I. Solomon, W. Nam, *J. Am. Chem. Soc.* 129 (2007) 1268–1277.
- [78] A. Takahashi, T. Kurahashi, H. Fujii, *Inorg. Chem.* 46 (2007) 6227–6229.
- [79] C. Hansch, A. Leo, R.W. Taft, *Chem. Rev.* 91 (1991) 165–195.
- [80] J. Shorter, *Pure Appl. Chem.* 69 (1997) 2497–2510.
- [81] N.W.J. Kamp, J.R.L. Smith, *J. Mol. Catal. A: Chem.* 113 (1996) 131–145.
- [82] S. Campestrini, A. Cagnina, *J. Mol. Catal. A: Chem.* 150 (1999) 77–86.
- [83] I.D. Cunningham, *Ann. Rep. Prog. Chem., Sect. B: Org. Chem.* 93 (1997) 27–41.
- [84] I.D. Cunningham, *Ann. Rep. Prog. Chem., Sect. B: Org. Chem.* 94 (1998) 273–288.
- [85] J. Clayden, N. Greeves, S. Warren, P. Wothers, *Organic Chemistry*, Oxford University Press, New York, 2001.
- [86] P.R. Ortiz de Montellano, *Cytochrome P450: Structure, Mechanism and Biochemistry*, third ed., Kluwer Academic/Plenum Publisher, New York, 2005.
- [87] W.J. Song, Y.O. Ryu, R. Song, W. Nam, *J. Biol. Inorg. Chem.* 10 (2005) 294–304.
- [88] Z. Pan, M. Newcomb, *Inorg. Chem.* 46 (2007) 6767–6774.
- [89] T.S. Lai, S.K.S. Lee, L.L. Yeung, H.Y. Liu, I.D. Williams, C.K. Chang, *Chem. Commun.* (2003) 620–621.
- [90] J.A.A.W. Elemans, E.J.A. Bijsterveld, A.E. Rowan, R.J.M. Nolte, *Eur. J. Org. Chem* (2007) 751–757.
- [91] D.V. Deubel, C. Loschen, G. Frenking, in: G. Frenking (Ed.), *Theoretical Aspects of Transition Metal Catalysis (Topics in Organometallic Chemistry)*, Springer-Verlag, Berlin, 2005, pp. 109–144.
- [92] K.A. Joergensen, B. Schioett, *Chem. Rev.* 90 (1990) 1483–1506.
- [93] M.C. Curet-Arana, R.Q. Snurr, L.J. Broadbelt, in: S.T. Oyama (Ed.), *Mechanism in Homogeneous and Heterogeneous Epoxidation Catalysis*, Elsevier, Amsterdam, 2008, pp. 471–486.